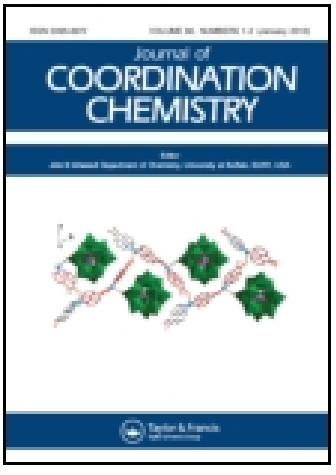

Journal of Coordination Chemistry
Publication details, including instructions for authors and subscription information:
http://www.tandfonline.com/loi/gcoo20

New fac-tricarbonyl rhenium(I) semicarbazone complexes: synthesis, characterization, and biological evaluation

Ignacio Machado[a], Soledad Fernández[b], Lorena Becco[c], Beatriz Garat[c], Jorge S. Gancheff[a], Ana Rey[b] & Dinorah Gambino[a]

[a] Facultad de Química, Cátedra de Química Inorgánica, Universidad de la República, Montevideo, Uruguay

[b] Facultad de Química, Cátedra de Radioquímica, Universidad de la República, Montevideo, Uruguay

[c] Laboratorio de Interacciones Moleculares, Facultad de Ciencias, Universidad de la República, Montevideo, Uruguay

Accepted author version posted online: 22 May 2014.Published online: 16 Jun 2014.

To cite this article: Ignacio Machado, Soledad Fernández, Lorena Becco, Beatriz Garat, Jorge S. Gancheff, Ana Rey & Dinorah Gambino (2014) New fac-tricarbonyl rhenium(I) semicarbazone complexes: synthesis, characterization, and biological evaluation, Journal of Coordination Chemistry, 67:10, 1835-1850, DOI: 10.1080/00958972.2014.926008

To link to this article: http://dx.doi.org/10.1080/00958972.2014.926008

Journal of Coordination Chemistry, 2014
Vol. 67, No. 10, 1835–1850, http://dx.doi.org/10.1080/00958972.2014.926008

New *fac*-tricarbonyl rhenium(I) semicarbazone complexes: synthesis, characterization, and biological evaluation

IGNACIO MACHADO†, SOLEDAD FERNÁNDEZ‡, LORENA BECCO§, BEATRIZ GARAT§, JORGE S. GANCHEFF†, ANA REY‡ and DINORAH GAMBINO*†

†Facultad de Química, Cátedra de Química Inorgánica, Universidad de la República, Montevideo, Uruguay
‡Facultad de Química, Cátedra de Radioquímica, Universidad de la República, Montevideo, Uruguay
§Laboratorio de Interacciones Moleculares, Facultad de Ciencias, Universidad de la República, Montevideo, Uruguay

(*Received 5 December 2013; accepted 4 April 2014*)

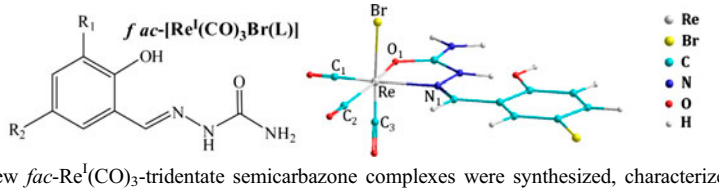

Five new *fac*-Re^{I}(CO)$_3$-tridentate semicarbazone complexes were synthesized, characterized and evaluated on *Trypanosoma cruzi*. The atypical bidentate coordination mode observed was supported by DFT calculations.

Expanding our previous work on salicylaldehyde semicarbazone metal complexes as prospective anti-trypanosomal agents, five new *fac*-Re^{I}(CO)$_3$-containing complexes with ligands of this semicarbazone series were synthesized and characterized. An atypical coordination mode of these potentially tridentate ligands through only the carbonylic oxygen and the azomethine nitrogen (the so-called N,O fashion) was demonstrated by IR spectroscopy and supported by theoretical calculations. Three of the compounds showed moderate *in vitro* anti-*Trypanosoma cruzi* activity and increased activity with respect to the corresponding free ligands. The brominated ligands, 5-bromo-2-hydroxybenzaldehyde semicarbazone (L2) and 5-bromo-2-hydroxy-3-methoxybenzaldehyde semicarbazone (L5), led to the most active rhenium(I) complexes. These compounds are among the few reported examples of rhenium complexes bearing *in vitro* activity against *T. cruzi*.

Keywords: Rhenium(I); Tricarbonyl complexes; *Trypanosoma cruzi*; Salicylaldehyde semicarbazones

1. Introduction

Besides increasing research on rhenium(I) carbonyl complexes due to their interesting photophysical, photochemical, and catalytic properties [1], the coordination chemistry of

*Corresponding author. Email: dgambino@fq.edu.uy

fac-$\{Re(CO)_3\}^+$ core has been widely explored for development of radiotherapeutic bioorganometallic agents for nuclear medicine purposes [2, 3].

Rhenium organometallics have been described as a new class of promising anti-proliferative compounds. Several tricarbonyl rhenium(I) complexes with interesting cytotoxicity on tumor cells have been reported and their mechanism of action has been explored [4]. In particular, some rhenium-based anti-tumor agents constitute promising candidates for clinical development [5].

During the last decade, our group has been devoted to the search for prospective anti-trypanosomal metal-based drugs by exploring different design strategies [6–8]. Chagas disease (American Trypanosomiasis), caused by *Trypanosoma cruzi* (*T. cruzi*), is one of the 17 diseases recognized by the World Health Organization as neglected illnesses [9]. It is endemic to Latin America where it affects around 10 million people mainly of poor areas and causes more deaths in this region than any other parasitic disease. Despite the efficacy of large-scale programs focused on insect vector control and on transfused blood testing, the disease could not be eradicated. Moreover, migration at the beginning of the 2000s caused the spread of the disease in non-endemic countries of North America and Europe. The current chemotherapy is based on two old drugs, Nifurtimox and Benznidazole. Both show several therapeutic disadvantages, like severe toxic effects and poor efficacy in the chronic phase of the disease. Hence, the development of more efficacious and less toxic drugs, which could also circumvent emerging drug resistance, is urgently needed [10–13].

As part of our research related with inorganic medicinal chemistry, we have developed several metal compounds of salicylaldehyde semicarbazone ligands (figure 1) [14–21]. In particular, oxidovanadium(IV) mixed-ligand complexes constitute promising candidates showing high anti-trypanosomal activity and very low unspecific cytotoxicity [19–21].

Although there are several reports on *fac*-tricarbonyl rhenium(I) thiosemicarbazone complexes, as far as we know only one very recent study deals with semicarbazone complexes [22–28]. Moreover, only the growth inhibitory effect on *T. cruzi* epimastigotes of Re(V) complexes with nitrofuryl semicarbazones has been previously evaluated [29]. In addition, rhenium complexes were little explored for anti-trypanosomal metal-based drug development. Fricker *et al.* tested a series of classical "3 + 1" mixed-ligand oxidorhenium(V) complexes including a tridentate and a monodentate ligand donor set and some of them showed *in vitro* inhibitory activity on the parasite [30]. Organometallic cyrhetrenyl complexes derived from 5-nitrofurane were recently *in vitro* evaluated on *T. cruzi* [31].

We decided to expand our previous work on salicylaldehyde semicarbazone complexes as prospective anti-trypanosomal agents by exploring the coordinative behavior of these ligands (figure 1) with the tricarbonylrhenium(I) core and the biological activity of the resulting organometallic compounds.

R_1	R_2	
H	H	L1
H	Br	L2
OCH_3	H	L3
OCH_2CH_3	H	L4
OCH_3	Br	L5

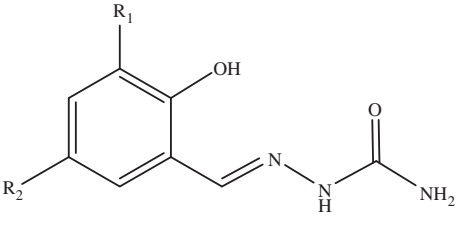

Figure 1. Tridentate salicylaldehyde semicarbazone derivatives selected as ligands.

2. Experimental setup

2.1. *Materials*

All common laboratory chemicals were purchased from commercial sources and used without purification. Semicarbazone ligands were synthesized from an equimolar mixture of the corresponding aldehyde and semicarbazide using a modification of a previously reported procedure and were characterized by C, H, and N elemental analyses; FTIR; and ^{1}H and ^{13}C NMR spectroscopy [14, 16–19]. The $[ReBr(CO)_5]$ precursor was prepared according to a published procedure by reacting $[Re_2(CO)_{10}]$ and Br_2 in hexane under N_2. Solid $[ReBr(CO)_5]$ was isolated by evaporating hexane at low pressure and was purified by sublimation [32, 33].

2.2. *Syntheses of the rhenium(I) complexes, $[Re^{I}(CO)_3Br(L)]$*

The new $[Re^{I}(CO)_3Br(L)]$ complexes, where L = salicylaldehyde semicarbazone (L1), 5-bromo-2-hydroxybenzaldehyde semicarbazone (L2), 2-hydroxy-3-methoxybenzaldehyde semicarbazone (L3), 2-hydroxy-3-ethoxybenzaldehyde semicarbazone (L4) or 5-bromo-2-hydroxy-3-methoxybenzaldehyde semicarbazone (L5), were prepared by mixing $[ReBr(CO)_5]$ (44 mg, 0.108 mM) with L (0.108 mM, 19 mg L1, 28 mg L2, 22 mg L3, 24 mg L4, 31 mg L5) in toluene (15 mL) and refluxing for 24 h. In each case, a gray solid was isolated by centrifugation and washed with two portions of toluene.

2.2.1. $[Re^{I}(CO)_3Br(L1)]$, 1. Yield: 32 mg, 56%. Anal. Calcd for $C_{11}H_9BrN_3O_5Re$ (%): C, 24.96; H, 1.71; N, 7.94. Found: C, 24.92; H, 1.79; N, 7.83. Λ_M(DMSO): 4.0 $Scm^2 M^{-1}$. ESI-MS (negative mode) (MeOH) *m/z* [Found (Calcd)]: 528.00 (527.92) $[M-H]^-$, 526.21 (525.92), 529.82 (529.92).

2.2.2. $[Re^{I}(CO)_3Br(L2)]$, 2. Yield: 45 mg, 68%. Anal. Calcd for $C_{11}H_8Br_2N_3O_5Re$ (%): C, 21.72; H, 1.33; N, 6.91. Found: C, 21.91; H, 1.35; N, 6.85. Λ_M(DMSO): 9.8 $Scm^2 M^{-1}$. ESI-MS (negative mode) (MeOH) *m/z* [Found (Calcd)]: 607.71 (607.83) $[M-H]^-$, 605.75 (605.83), 609.69 (609.83), 603.74 (603.83).

2.2.3. $[Re^{I}(CO)_3Br(L3)]$, 3. Yield: 53 mg, 88%. Anal. Calcd for $C_{12}H_{11}BrN_3O_6Re$ (%): C, 25.77; H, 1.98; N, 7.51. Found: C, 25.61; H, 2.00; N, 7.41. Λ_M(DMSO): 5.7 $Scm^2 M^{-1}$. ESI-MS (negative mode) (MeOH) *m/z* [Found (Calcd)]: 557.90 (557.90) $[M-H]^-$, 559.80 (559.90), 556.00 (555.90).

2.2.4. $[Re^{I}(CO)_3Br(L4)]$, 4. Yield: 48 mg, 78%. Anal. Calcd for $C_{13}H_{13}BrN_3O_6Re$ (%): C, 27.23; H, 2.29; N, 7.33. Found: C, 27.37; H, 2.22; N, 7.28. Λ_M(DMSO): 6.2 $Scm^2 M^{-1}$. ESI-MS (negative mode) (MeOH) *m/z* [Found (Calcd)]: 571.93 (571.94) $[M-H]^-$, 573.79 (573.94), 570.05 (569.94).

2.2.5. [$Re^{I}(CO)_3Br(L5)$], 5. Yield: 22 mg, 32%. Anal. Calcd for $C_{12}H_{10}Br_2N_3O_6Re$ (%): C, 22.58; H, 1.58; N, 6.58. Found: C, 22.76; H, 1.60; N, 6.46. Λ_M(DMSO): 3.7 $Scm^2\,M^{-1}$. ESI-MS (negative mode) (MeOH) *m/z* [Found (Calcd)]: 637.70 (637.84) $[M-H]^-$, 639.99 (639.85), 635.66 (635.80), 633.75 (633.90).

2.3. *Physicochemical characterization*

C, H, and N analyses were performed with a Thermo Flash 2000 elemental analyzer. Mass spectrometry of methanolic solutions of the complexes was performed on an Ion Trap mass spectrometer Bruker Esquire 6000 equipped with an electrospray ionization source and operated in the negative-ion mode. Conductometric measurements were performed at 25 °C in 10^{-3} M DMSO solutions using a Conductivity Meter 4310 Jenway [34]. FTIR spectra (4000–400 cm^{-1}) of the complexes and the free ligands were measured as KBr pellets with a Bomen FTIR model M102 instrument. ^{1}H NMR spectra of the free ligands and complexes were recorded on a Bruker DPX-400 instrument (at 400 MHz). Experiments were performed at 30 °C in DMSO-d_6. Heteronuclear correlation experiments (2-D-HETCOR), heteronuclear multiple quantum correlation and heteronuclear multiple bond correlation, were performed with the same instrument.

2.4. *Computational studies*

All computational studies have been undertaken at the density functional level of theory (DFT). The geometries of the complexes were optimized in a closed-shell singlet ($S = 1$). The absence of crystallographic data prompted us to conduct stability studies of the isomers derived from the different coordination positions of bromide, and from two bidentate coordination modes of the ligand. Their optimizations were conducted with B3LYP [35] in combination with LANL2DZ [36, 37]. For the most stable configuration, studies on equilibrium geometry were performed by employing PBE1PBE [38] in combination with the so-called STMIDI basis set (see below for details). PBE1PBE/STMIDI has proven to adequately describe geometries of large complexes at a very low computational cost [39–42]. The valence electrons for non-metal atoms in STMIDI were treated with MIDI! [43], those for the metal being described by a basis set (8s7p6d2f1g)/[6s5p3d2f1g] [44]. The core electrons were replaced by Stuttgart effective-core pseudo-potentials [44, 45]. LANL2DZ and STMIDI take scalar relativistic effects into account, especially important when systems with heavy atoms are studied [46]. The nature of the stationary point was verified through a vibrational analysis (no imaginary frequencies). All theoretical studies reported in this work were conducted by employing the program package Gaussian 09, Rev. A.01 [47].

2.5. *Biological activity*

2.5.1. *In vitro* anti-*T. cruzi* activity. *T. cruzi* epimastigotes of the Dm28c strain were maintained in exponential growth at 28 °C in liver infusion tryptose medium complemented with 10% (v/v) fetal calf serum. The effect on cell growth was analyzed incubating an initial concentration of 1×10^6 cells mL^{-1} with various concentrations of the compounds for five days. Compounds were added as stock DMSO solutions immediately after the preparation of these solutions. The final DMSO concentration in the culture media never exceeded 0.4% (v/v) and had no effect by itself on the proliferation of the parasites [19, 20]. The

percentage of cell growth was followed by measuring the absorbance, A, of the culture at 595 nm and calculated as follows: % = $(Ap - A_0p)/(Ac - A_0c) \times 100$, where $Ap = A_{595}$ of the culture containing the drug at day 5; $A_0p = A_{595}$ of the culture containing the drug at day 0; $Ac = A_{595}$ of the culture in the absence of any drug (control) at day 5; and $A_0c = A_{595}$ in the absence of the drug at day 0. Dose-response curves were recorded and the IC_{50} values (50% inhibitory concentration) were determined. The results are presented as averages ± standard deviation (SD). Nifurtimox (Nfx) was used as the reference trypanosomicidal drug.

2.6. *Lipophilicity studies*

Reversed-phase TLC experiments were done on pre-coated TLC plates SIL RP-18W/UV_{254} and eluted with MeOH : DMF : 10 mM aqueous buffer Tris pH 7.4 (20 : 20 : 60 v/v/v). Stock solutions were prepared in pure methanol (Aldrich) prior to use. The plates were developed in a closed chromatographic tank, dried, and the spots were located under UV light. The R_f values were averaged from two to three determinations and converted to R_M via the relationship: $R_M = \log_{10}[(1/R_f) - 1]$ [19, 20, 48, 49].

3. Results and discussion

Five complexes of the tridentate salicylaldehyde semicarbazone derivatives L1–L5 (figure 1) were synthesized with good yields. Attempts to obtain single crystals for performing X-ray diffraction studies failed. All the complexes are non-conducting in DMSO, indicative of the presence of neutral species. Analytical, ESI-MS, FTIR, and ^{1}H NMR spectroscopic results are in agreement with the proposed formula, $[Re^I(CO)_3Br(L)]$. ESI-MS experiments allowed the clear detection of the $[M-H]^-$ species for each Re-complex. In all cases, peaks reflecting the isotope distribution of ^{79}Br and ^{81}Br were detected in agreement with the presence of one (complexes **1**, **3** and **4**) or two (complexes **2** and **5**) bromine atoms per molecule.

Numerous Re(I)-based complexes described in the literature were prepared via displacement of two carbonyls of the Re(I)-pentacarbonyl complexes $[Re(CO)_5X]$, where X = Cl or Br, by bidentate ligands bearing various donors (O, S, Se, Te, N, and P). In these cases, the three carbonyl ligands of the kinetically inert $\{Re(CO)_3\}^+$ core served to fix three coordination sites, leaving available three positions for ligand substitution. Moreover, different ligands, like some thiosemicarbazones, were able to displace two carbonyl groups but also the bromide acting as tridentate ligands [50, 51]. The salicylaldehyde semicarbazones selected in this work have demonstrated their ability to act as tridentate ligands of different metal ions through the azomethine nitrogen, carbonyl oxygen, and the phenolic oxygen (figure 1) [14–21]. We were interested in expanding our previous chemical work by studying the coordination behavior of L1–L5 towards the $\{Re(CO)_3\}^+$ core. All the results show that in this case the ligands were not able to coordinate tridentate, leading to $[Re^I(CO)_3Br(L)]$ species instead of $[Re^I(CO)_3(L–H)]$ ones.

3.1. *IR spectroscopic studies*

Based on our previous experience for vibrational behavior of metal complexes of salicylaldehyde semicarbazone derivatives [14–21], vibration bands related to the semicarbazone

coordination mode were tentatively assigned. Some selected vibration bands and their tentative assignments are presented in table 1. The absence of the ν(C=O) bands, present in the ligands at 1667–1698 cm^{-1}, and the appearance of strong bands at ca. 1646–1655 cm^{-1} are characteristic of the coordination of these ligands through carbonylic oxygen [52].

The shift of ν(C=O) and ν(C=N) bands and the presence of ν(OH) (in the 3420–3480 cm^{-1} region) are in agreement with bidentate coordination through the carbonylic oxygen ($O_{O-C(NH2)=N}$) and the azomethine nitrogen ($N_{azomethine}$) [14–21].

The IR spectra display three strong carbonyl stretching bands, ν(C≡O), in the 2034–1898 cm^{-1} region, which are characteristic of monomeric pseudo-octahedral *fac*-$\{Re(CO)_3\}^+$ complexes [53–56].

3.2. *NMR results*

NMR spectroscopic data show narrow signals, typical of diamagnetic complexes. HETCOR experiments allow assigning all ^{1}H signals. ^{1}H NMR integrations and signal multiplicities are in line with the proposed formula. Table 2 includes the ^{1}H NMR chemical shift values along with chemical shift differences between each complex and the corresponding ligand (expressed as $\Delta\delta$). The figure included in table 2 shows the numbering scheme of the salicylaldehyde semicarbazone moiety used as a general numbering scaffold for the five selected ligands either in the table or in the text. The five complexes show similar ^{1}H chemical shifts of the salicylaldehyde semicarbazone fragment. As previously discussed for gallium(III) and dioxidovanadium(V) complexes of these ligands, upon coordination the deshielding effect of the metal is apparent in some protons near the nitrogen and carbonylic oxygen donors (i.e. protons 8, 10 and 11), causing a downfield shift of the corresponding ^{1}H NMR signals [14, 15, 20]. Nevertheless, almost all protons are affected due to coordination to the rhenium core.

3.3. *Computational studies*

3.3.1. Geometries and isomer stability. The experimental results are in line with the presence of a neutral complex with bidentate semicarbazone derivative (L), which can, in principle, lead to two coordination modes (labeled as "N,O" and "N,OH", respectively)

Table 1. Tentative assignment of selected IR bands of the $[Re^I(CO)_3Br(L)]$ complexes **1–5**. Bands of the free semicarbazone ligands L1–L5 are included for comparison [14–21]. Band positions are given in cm^{-1}.

Compound	ν(C=O)	ν(C=N)[a]	ν(O–H)	ν(N–H)	ν(C≡O)
L1	1695	1593	3493	3157	–
$[Re^I(CO)_3Br(L1)]$, **1**	1655	1555	3459	3200	2032, 1945 sh,1929
L2	1698	1596	3470	3191	–
$[Re^I(CO)_3Br(L2)]$, **2**	1655	1553	3448	3170	2034, 1918 br
L3	1676	1586	3466	3171	–
$[Re^I(CO)_3Br(L3)]$, **3**	1650	1553	3450	3157	2028, 1914, 1888
L4	1667	1595	3433	3160	–
$[Re^I(CO)_3Br(L4)]$, **4**	1648	1555	3420	3152	2032, 1916, 1899
L5	1672	1572	3477	3190	–
$[Re^I(CO)_3Br(L5)]$, **5**	1646	1540	3480	3162	2027, 1920, 1898

[a]The bands assigned to ν(C=N) (azomethine) are associated with other stretching bands [20, 21, 45].

Table 2. ^{1}H NMR chemical shifts (δ, ppm) of the [$Re^{I}(CO)_3Br$(L)] complexes and the L ligands in DMSO-d_6 at 30 °C.

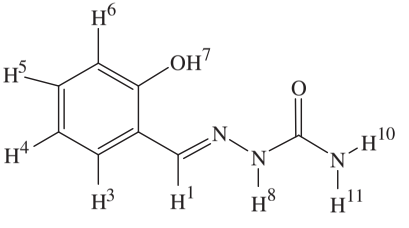

	[$Re^{I}(CO)_3Br$(L1)]			[$Re^{I}(CO)_3Br$(L2)]			[$Re^{I}(CO)_3Br$(L3)]			[$Re^{I}(CO)_3Br$(L4)]			[$Re^{I}(CO)_3Br$(L5)]		
H	δ_{ligand}	$\delta_{complex}$	$\Delta\delta^a$	δ_{ligand}	$\delta_{complex}$	$\Delta\delta^a$	δ_{ligand}	$\delta_{complex}$	$\Delta\delta^a$	δ_{ligand}	$\delta_{complex}$	$\Delta\delta^a$	δ_{ligand}	$\delta_{complex}$	$\Delta\delta^a$
1	8.15	8.56	0.41	8.07	8.49	0.42	8.17	8.04	−0.13	8.17	8.02	−0.15	8.11	8.52	0.39
3	7.75	7.79	0.04	8.05	8.07	0.02	7.38	7.24	−0.14	7.34	7.26	−0.08	7.69	7.59	−0.10
4	6.83	7.37	0.54	–	–	–	6.77	7.12	0.35	6.75	7.09	0.34	–	–	–
5	7.16	7.75	0.59	7.28	7.96	0.68	6.92	7.17	0.25	6.92	7.16	0.24	7.06	7.30	0.24
6	6.87	7.39	0.52	6.80	7.52	1.02	–	–	–	–	–	–	–	–	–
7	9.97	na	–	10.22	10.74	0.52	9.30	10.50	1.20	9.19	na	–	9.47	10.06	0.59
8	10.20	12.57	2.37	10.26	12.70	2.43	10.22	12.57	2.35	10.21	12.58	2.37	10.28	12.65	2.37
10,11	6.42	6.92	0.50	6.55	6.90	0.35	6.41	6.94	0.53	6.41	6.92	0.51	6.53	6.64	0.11
CH_3	–	–	–	–	–	–	3.80	3.83	0.03	1.35	1.37	0.02	3.83	3.87	0.02
CH_2	–	–	–	–	–	–	–	–		4.06	4.11	0.05	–	–	

[a] $\Delta\delta = \delta_{complex} - \delta_{ligand}$; na: not assigned.

(figure 2). The different coordination positions of the halide lead to the isomers displayed in figures 3 and 4 (for the particular case of $[Re(CO)_3Br(L2)]$): *fac*-isomer (**1**) and *mer*-isomers (**2** and **3**), results for only one of the *fac*-enantiomers are presented and discussed.

The optimization for all isomers has been conducted with B3LYP/LANL2DZ, which gives a minimum stationary point in all cases. The stability results point to *fac*-isomer being the most stable with L2 ($R_1 = H$; $R_2 = Br$) coordinating rhenium in either mode (see figure 2). The largest energy differences between isomers are observed for the ones featuring bromide in an in-plane coordination position, regardless of the coordination mode of L2. When L2 coordinates N,O to rhenium ($L2_{N–O}$), the calculated energy difference is 22 kcal M^{-1} (isomer 3), while in a N,OH-mode ($L2_{N–OH}$) the difference is 26 kcal M^{-1} (isomer 2).

In studying the stability of the *fac*-stereoisomer 1 with $L2_{N–O}$ and with $L2_{N–OH}$, calculations show the first to be more stable than the second one by 9 kcal M^{-1}. This energy difference is the result of conformational changes in the semicarbazone, changes in the chelate ring size and the formation of an intra-ligand N–H···O hydrogen bond when L coordinates rhenium in a N,O-mode. The results of the Gibbs energy are also in line with the above-mentioned stability results.

These findings are consistent with the coordination mode exhibited by other salicylaldehyde semicarbazone derivatives in rhenium(I) tricarbonyl complexes [28]. A different behavior was previously reported for a $[Re(CO)_3Br(L)]$ complex of a potentially tridentate thiosemicarbazone N,N,S ligand (L) that coordinated in a bidentate mode through both nitrogen donors but not through its thiocarbonylic sulfur donor site [50].

Regarding the carbonyl ligands, we are not aware of a *mer*-configuration of the carbonyl ligands in tricarbonyl-based complexes of rhenium(I). Our results of isomer stability (table 3) for $[Re(CO)_3Br(L2)]$ are also in agreement with this observation. Therefore, we expect to obtain $[Re(CO)_3Br(L2)]$ as a racemic mixture.

Besides study of the electronic features of the most stable isomers of $[Re(CO)_3Br(L2)]$, it is also our aim to test the reliability of PBE1PBE/STMIDI in studying the electronic properties of complexes with rhenium in low oxidation states. Therefore, we decided to investigate the geometry and the vibrational IR spectrum for *fac*-$[Re(CO)_3Br(L2)]$ (**1** in figures 3 and 4) with PBE1PBE/STMIDI.

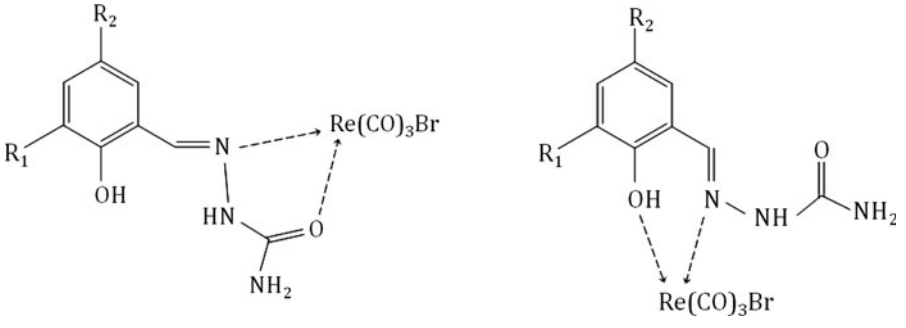

Figure 2. Bidentate coordination possibilities of the semicarbazone employed in this work: N,O-mode (left) and the N,OH-mode (right).

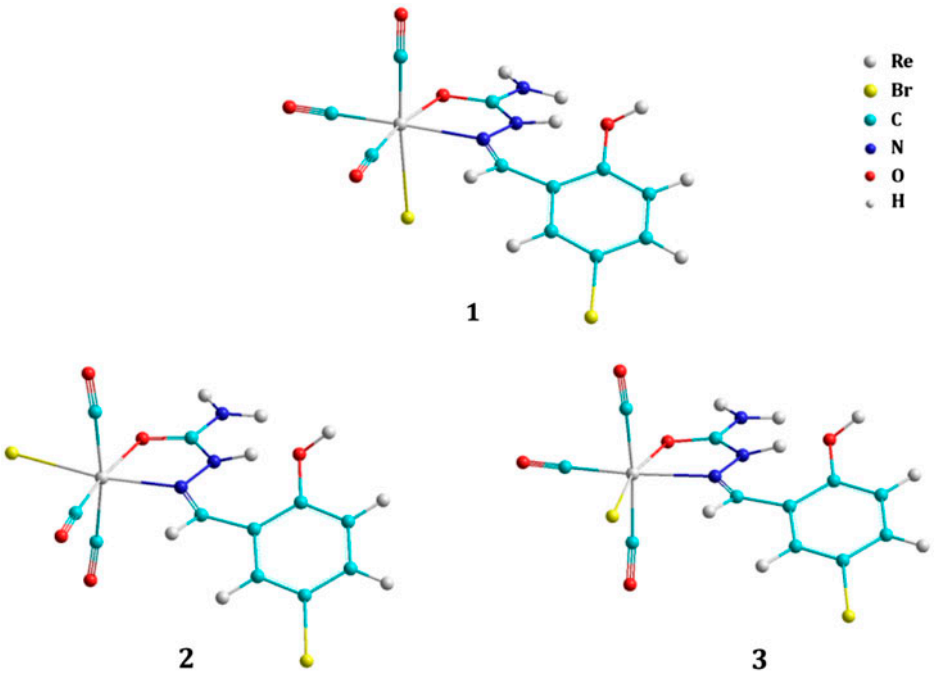

Figure 3. Optimized structures of the isomers of $[Re(CO)_3Br(L2)]$ derived from the different coordination positions of the halide ligand in a N,O coordination mode of L2 by employing B3LYP/LANL2DZ.

To elucidate the coordination mode of the semicarbazones considered in this work, we studied the vibrational IR spectrum of the most stable isomer of $[Re(CO)_3Br(L2)]$ by employing PBE1PBE/STMIDI. The calculated vibrational IR spectra for the *fac*-isomer 1 with $L2_{N–O}$ and with $L2_{N–OH}$ are depicted in figure 5, in which the experimental one is also included.

The better simulation of the IR spectrum is obtained for the complex with $L2_{N–O}$. The most important difference arises in the region between 2100 and 1500 cm^{-1}, in which the stretching mode of C=O is presented. The calculations allow us to distinguish C=O coordinating rhenium (N,O-mode) from uncoordinated C=O (N,OH-mode). While calculated ν(C=O) in the first case appears at 1735 cm^{-1} (shifted +37 cm^{-1} with respect to the experimental value), it is calculated at 1862 cm^{-1} for L coordinating rhenium in a N,OH-mode. Therefore, from the comparison of the theoretical and the experimental band pattern from 2100 to 1500 cm^{-1} for the complex with $L2_{N–O}$, and taking the origin of these bands as mentioned above into account, we are in the position to assume that L2 is a bidentate ligand coordinating through the carbonylic oxygen and the azomethine nitrogen.

The calculated spectrum of $[Re(CO)_3Br(L2_{N–O})]$ exhibits a very intense band at 2086 cm^{-1}, attributable to ν(C≡O) of the carbonyl ligands, which is simulated at +52 cm^{-1} shifted with respect to the experimental value. In the low-energy part of the spectrum, the stretching of the carbonyl groups leads to two very intense bands simulated at 2010 and 1983 cm^{-1}, which can be related to the broad band experimentally detected at 1918 cm^{-1}. It is worth mentioning that this broad band has been observed as two independent bands for

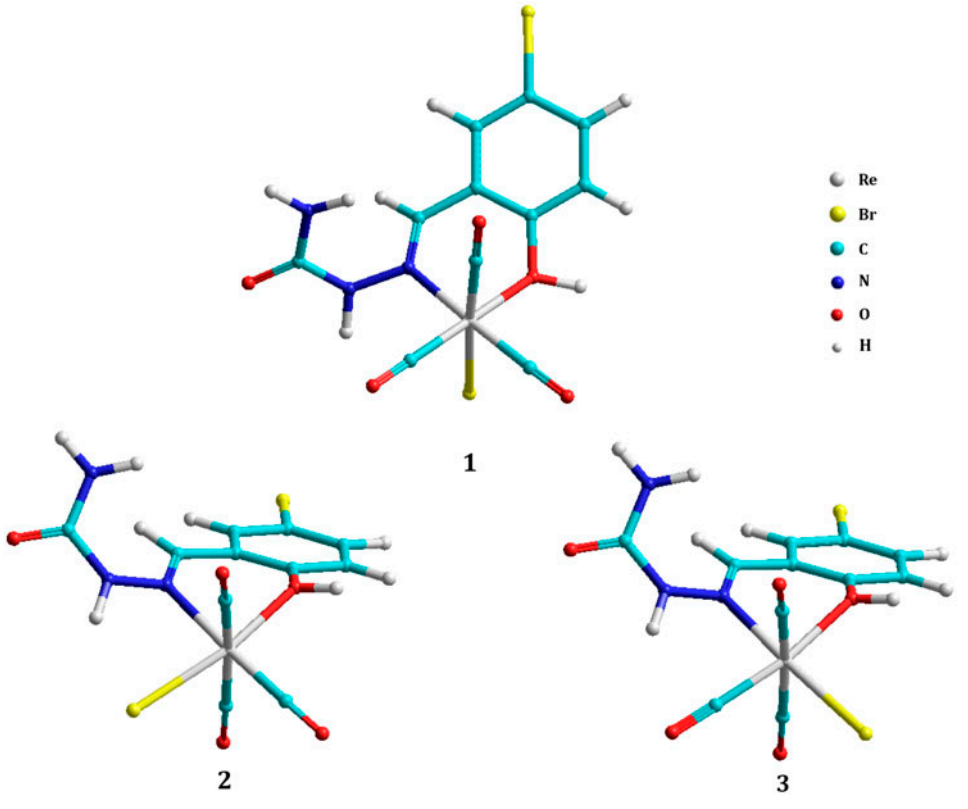

Figure 4. Optimized structures of the isomers of $[Re(CO)_3Br(L2)]$ derived from the different coordination positions of the halide ligand in a N,OH coordination mode of L2 by employing B3LYP/LANL2DZ.

Table 3. Energy difference between isomers of $[Re(CO)_3Br(L2)]$ as computed with B3LYP/LANL2DZ (in the gas phase) taking two coordination modes of L into account ($T = 298$ K).

Coordination mode	Isomer #	ΔE (kcal M^{-1})[a]	$\Delta G°$ (kcal M^{-1})[a]
N,O	1	0[b]	0[d]
	2	21	21
	3	22	22
N,OH	1	0[c]	0[e]
	2	26	26
	3	15	15

[a]Energy difference with respect to the most stable isomer.
[b]E isomer # 1 (N,O-coordination mode) = –1069.81063729 u.a.
[c]E isomer # 1 (N,OH-coordination mode) = –1069.7961849 u.a.
[d]G isomer # 1 (N,O-coordination mode) = –1069.79618492 u.a.
[e]G isomer # 1 (N,OH-coordination mode) = –1069.57021273 u.a.

all the other complexes included in this work. At 1734 and 1601 cm^{-1}, two intense bands, ascribable to ν(C=O) + $\delta(NH_2)$ and ν(C=N) + $\delta(NH_2)$, respectively, have also been calculated. Both bands are shifted with respect to the experimental evidence, the shifts

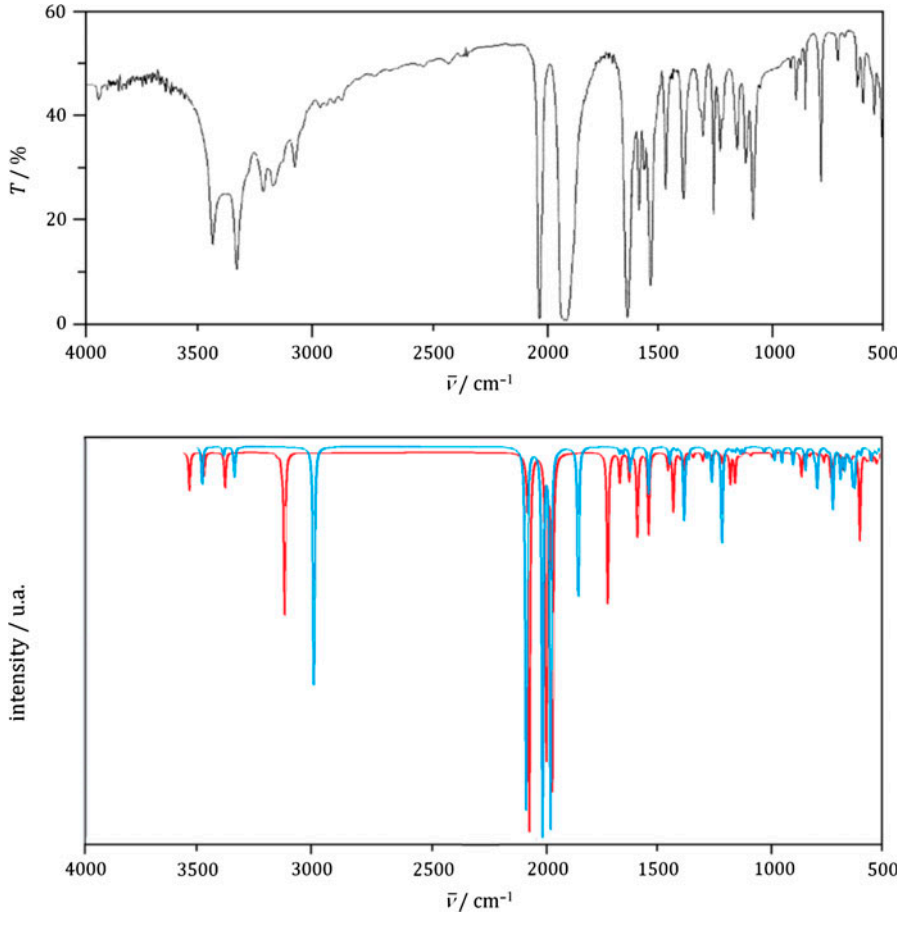

Figure 5. Experimental vibrational IR spectra of [$Re(CO)_3Br(L2)$] (top), and theoretical (bottom) as calculated with PBE1PBE/STMIDI for the most stable isomer in a N,O-coordination mode of L2 (red line), and in a N,OH-mode of L2 (blue line) (see http://dx.doi.org/10.1080/00958972.2014.926008 for color version).

being +36 and +51 cm^{-1}, respectively. All findings already commented on are in line with the conclusion that [$Re(CO)_3Br(L2_{N-O})$] is obtained in the solid state as a racemic mixture of stereoisomers 1 and 2. Optimized geometry of isomer 1 is displayed in figure 6. Selected optimized parameters are gathered in table 4.

The calculated structure of *fac*-[$Re(CO)_3Br(L2_{N-O})$] with PBE1PBE/STMIDI exhibits a slightly distorted octahedral rhenium ion featured by metric parameters in good agreement with the ones recently reported for the related [$Re(CO)_3Br(H_2Bu_2)$] (H_2Bu_2 = salicylaldehyde-*N*,*N*-dibutyl semicarbazone) [28]. The geometry at the minimum displays Re–C bond lengths ranging from 1.891 to 1.917 Å (exp. value of 1.90 Å). All other calculated Re-non-metal bond lengths show a deviation of up to 0.051 Å (Re–Br), which account for a good performance of PBE1PBE/STMIDI in dealing with optimized structures of complexes with rhenium in oxidation state +1.

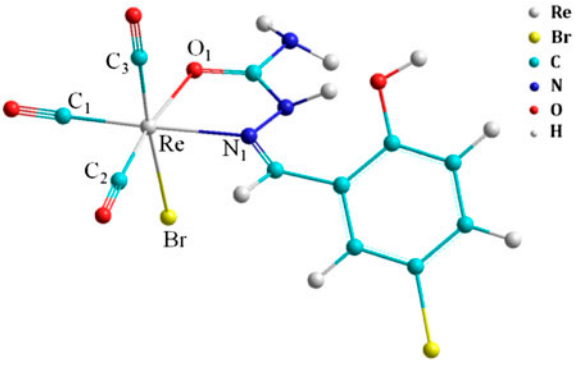

Figure 6. Most stable isomer of $[Re(CO)_3Br(L2_{N-O})]$ as calculated with PBE1PBE/STMIDI ($T = 298$ K).

Table 4. Selected geometric parameters calculated for the most stable isomer of $[Re(CO)_3Br(L2_{N-O})]$ by using PBE1PBE/STMIDI ($T = 298$ K).[a]

Complex	Bond	d (Å)	Angle	∠ (°)
fac-$[Re(CO)_3Br(L2_{N-O})]$	$Re–C_1$	1.917	$C_1–Re–C_2$	88.3
	$Re–C_2$	1.891	$C_1–Re–O_1$	98.9
	$Re–C_3$	1.905	$C_2–Re–N_1$	98.6
	Re–Br	2.564	$O_1–Re–N_1$	74.1
	$Re–N_1$	2.182	$Br–Re–N_1$	82.9
	$Re–O_1$	2.186	$Br–Re–C_1$	93.3

[a]For atom assignment see figure 6.

Table 5. *In vitro* biological activity on *T. cruzi* (Dm28c strain) and lipophilicity of the *fac*-$Re(CO)_3$-containing complexes. Nifurtimox and $[Re(CO)_5Br]$ were included for comparison.

Compound	$IC_{50} \pm SD$ (μM)[a]	R_M[b]
$[Re^I(CO)_3BrL1]$, **1**	67.1 ± 1.3	–0.35
$[Re^I(CO)_3BrL2]$, **2**	57.3 ± 8.7	–0.05
$[Re^I(CO)_3BrL3]$, **3**	168.1 ± 40.8	–0.54
$[Re^I(CO)_3BrL4]$, **4**	187.0 ± 31.4	–0.31
$[Re^I(CO)_3BrL5]$, **5**	59.9 ± 3.8	–0.09
L1	>100 [15, 18]	–0.57
L2	>100 [15, 18]	–0.07
L3	>100 [15, 18]	–0.71
L4	>100 [15, 18]	–0.66
L5	>100 [15, 18]	–0.09
$[Re(CO)_5Br]$	107.6 ± 15.2	–
Nifurtimox	6.0 [18]	–

[a]IC_{50}: concentration that inhibits 50% of the parasite growth, SD: standard deviation.
[b]$R_M = \log_{10}[(1/R_f) - 1]$.

3.4. *Biological activity*

3.4.1. *In vitro* anti-*T. cruzi* activity. The complexes were *in vitro* evaluated for their anti-*T. cruzi* activities against the epimastigote form (Dm28c strain). The results were compared to that of the reference drug Nifurtimox (table 5). The free semicarbazones L1–L5 have been previously tested by the same *in vitro* test and have shown no significant inhibitory

effect on *T. cruzi* epimastigotes ($IC_{50} > 100\ \mu M$) [16, 19]. The precursor $[Re(CO)_5Br]$ was also tested for comparison. It shows very low activity on the parasite.

The L1, L2, and L5 new rhenium(I) complexes show moderate activity on *T. cruzi* epimastigotes. An improvement of the anti-trypanosomal activity is observed upon coordination to rhenium. Both brominated ligands, L2 and L5, lead to the most active rhenium(I) complexes. Similar enhanced bioactivity has been previously reported for the gallium(III) and oxidovanadium(IV) complexes of these salicylaldehyde semicarbazone derivatives [18, 21].

3.5. *Lipophilicity studies*

Lipophilic, polar, electronic, and steric effects are among the prime factors controlling transport to and interaction with biological receptors. Hence, structure–activity relationships usually involve studying the effect of lipophilicity, among other factors, on biological activity [20, 21, 57]. Therefore, this physicochemical property was determined for the whole series of the newly developed *fac*-$Re^{I}(CO)_3$-based complexes trying to find out if bioactivity is correlated with this factor.

Lipophilicity was experimentally determined using reversed-phase TLC experiments where the stationary phase, precoated TLC-C_{18}, may be considered to simulate lipids of

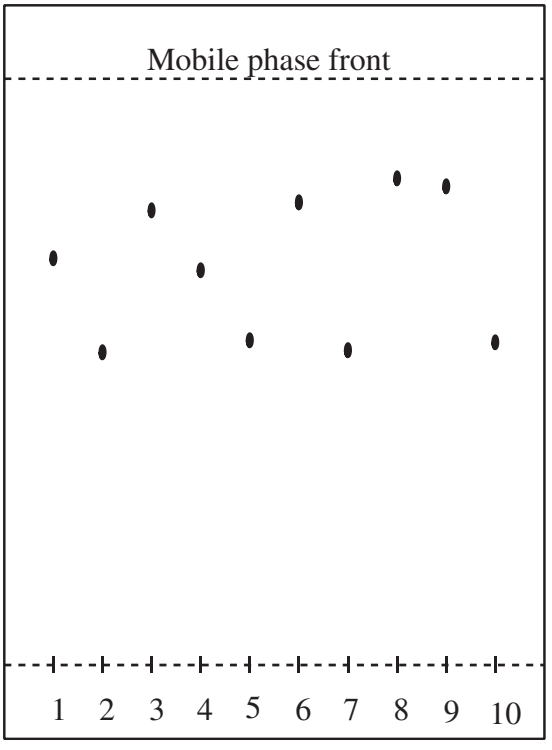

Figure 7. Schematic representation of the lipophilicity determination by TLC (see text): 1: complex **1**, $R_f = 0.69$; 2: complex **2**, $R_f = 0.53$; 3: complex **3**, $R_f = 0.78$; 4: complex **4**, $R_f = 0.67$; 5: complex **5**, $R_f = 0.55$; 6: L1, $R_f = 0.79$; 7: L2, $R_f = 0.54$; 8: L3, $R_f = 0.83$; 9: L4, $R_f = 0.82$; 10: L5, $R_f = 0.56$.

biological membranes or receptors, and the mobile phase, MeOH : DMF : Tris–HCl buffer pH 7.4 (20 : 20 : 60, v/v/v), resembles the aqueous biological milieu. The composition of the mobile phase was modified and adjusted in order to allow differentiating complexes according to their lipophilicity (figure 7). The most adequate one was a combination of polar organic solvents, MeOH and DMF, together with a buffer that simulates the physiological pH value. Table 5 summarizes the R_M values for each complex together with those values determined for the free ligands in the same experiment.

Each Re–L complex shows a lower R_f value than the corresponding free ligand L. That means that, as expected, each rhenium(I) tricarbonyl complex is more lipophilic than the free ligand. Nevertheless, only three complexes of five are more active than the free ligands. Although a significantly higher number of complexes would be needed in order to establish a more reliable conclusion, no apparent correlation could be observed between lipophilicity of the complexes and their anti-trypanosomal activities. At this stage, we conclude that other physicochemical factors or a combination of factors including lipophilicity could determine the activity tendency experimentally observed. Work is in progress to increase the number of structurally related Re(I) tricarbonyl compounds by modification of the substitution pattern on the salicylaldehyde semicarbazone moiety in order to determine structure–activity relationships and improve the biological activity.

4. Conclusion

Five new *fac*-$Re^{I}(CO)_3$-containing complexes with salicylaldehyde derivatives as ligands were synthesized and characterized. The potentially tridentate semicarbazone ligands showed an atypical bidentate coordination mode through the carbonylic oxygen and the azomethine nitrogen. This observation was supported by DFT calculations. Studies on the equilibrium geometry performed with B3LYP/LANL2DZ pointed to the isomer featured by an out-of-plane coordinated bromide (in either coordination modes of L) to be the most abundant one. The vibrational IR spectrum computed with PBE1PBE/STMIDI has proven to be useful for studying the features of the coordination sphere, in which semicarbazone is bidentate by employing the carbonylic oxygen and the azomethine nitrogen as donors. Calculated metric parameters for the optimized structure were in agreement with those reported for the X-ray-determined structure of $[Re(CO)_3Br(H_2Bu_2)]$ (H_2Bu_2 = salicylaldehyde-*N*, *N*-dibutyl semicarbazone). Thus, PBE1PBE in combination with STMIDI could be confidently employed in studying complexes of Re(I) with semicarbazone-derivative ligands keeping the computational cost very low.

Three of the new compounds showed moderate anti-*T. cruzi* activity and increased activity with respect to the corresponding free ligands. These are among the few reported examples of rhenium complexes bearing *in vitro* activity against *T. cruzi*.

Acknowledgements

IM thanks ANII-Uruguay for a research grant [grant number INI_X_2011_1_3902]. Authors would like to thank T Possi and Dr A Rodríguez for MS analysis (Polo Tecnológico-Facultad de Química, UdelaR, EU Grant "Proyecto Enlaces-UE URY 2003-5906").

References

[1] Y. Kuninobu, K. Takai. *Chem. Rev.*, **111**, 1938 (2011).
[2] R. Alberto, R. Schibli, R. Waibel, U. Abram, A.P. Schubiger. *Coord. Chem. Rev.*, **190–192**, 901 (1999).
[3] (a) N. Metzler-Nolte. *Angew. Chem. Int. Ed.*, **40**, 1040 (2001); (b) N. Lazarova, S. James, J. Babich, J. Zubieta. *Inorg. Chem. Commun.*, **7**, 1023 (2004).
[4] G. Gasser, I. Ott, N. Metzler-Nolte. *J. Med. Chem.*, **54**, 3 (2011).
[5] A.V. Shtemenko, P. Collery, N.I. Shtemenko, K.V. Domasevitch, E.D. Zabitskaya, A.A. Golichenko. *Dalton Trans.*, 5132 (2009).
[6] D. Gambino, L. Otero. *Inorg. Chim. Acta*, **393**, 103 (2012).
[7] M. Navarro, G. Gabbiani, L. Messori, D. Gambino. *Drug Discovery Today*, **15**, 1070 (2010).
[8] D. Gambino. *Coord. Chem. Rev.*, **255**, 2193 (2011).
[9] Available online at: http://www.who.int/neglected_diseases/diseases/en/(consulted22September2013).
[10] I. Ribeiro, A.M. Sevcsik, F. Alves, G. Diap, R. Don, M.O. Harhay, S. Chang, B. Pecoul. *PLoS Negl. Trop. Dis.*, **3**, e484 (2009). doi:10.1371/journal.pntd.0000484.
[11] J.A. Urbina. *Drugs Future*, **35**, 409 (2010).
[12] P.J. Hotez, D.H. Molyneux, A. Fenwick, J. Kumaresan, S. Ehrlich Sachs, J.D. Sachs, L. Savioli. *N. Engl. J. Med.*, **357**, 1018 (2007).
[13] J.D. Maya, B.K. Cassels, P. Iturriaga-Vásquez, J. Ferreira, M. Faúndez, N. Galanti, A. Ferreira, A. Morello. *Comp. Biochem. Physiol. Part A: Physiol.*, **146**, 601 (2007).
[14] P. Noblía, E.J. Baran, L. Otero, P. Draper, H. Cerecetto, M. González, O.E. Piro, E.E. Castellano, T. Inohara, Y. Adachi, H. Sakurai, D. Gambino. *Eur. J. Inorg. Chem.*, **2**, 322 (2004).
[15] P. Noblía, M. Vieites, B. Parajón-Costa, E.J. Baran, H. Cerecetto, P. Draper, M. González, O.E. Piro, E.E. Castellano, A. Azqueta, A. López, A. Monge-Vega, D. Gambino. *J. Inorg. Biochem.*, **99**, 443 (2005).
[16] J. Benítez, L. Guggeri, I. Tomaz, G. Arrambide, M. Navarro, J. Costa Pessoa, B. Garat, D. Gambino. *J. Inorg. Biochem.*, **103**, 609 (2009).
[17] J. Rivadeneira, D. Barrio, G. Arrambide, D. Gambino, L. Bruzzone, S. Etcheverry. *J. Inorg. Biochem.*, **103**, 633 (2009).
[18] D. Gambino, M. Fernández, D. Santos, G.A. Etcheverría, O.E. Piro, F.R. Pavan, C.Q.F. Leite, I. Tomaz, F. Marques. *Polyhedron*, **30**, 1360 (2011).
[19] J. Benítez, L. Becco, I. Correia, S. Milena Leal, H. Guiset, J. Costa Pessoa, J. Lorenzo, S. Tanco, P. Escobar, V. Moreno, B. Garat, D. Gambino. *J. Inorg. Biochem.*, **105**, 303 (2011).
[20] M. Fernández, L. Becco, I. Correia, J. Benítez, O.E. Piro, G.A. Echeverria, A. Medeiros, M. Comini, M.L. Lavaggi, M. González, H. Cerecetto, V. Moreno, J. Costa Pessoa, B. Garat, D. Gambino. *J. Inorg. Biochem.*, **127**, 150 (2013).
[21] M. Fernández, J. Varela, I. Correia, E. Birriel, J. Castiglioni, V. Moreno, J. Costa Pessoa, H. Cerecetto, M. González, D. Gambino. *Dalton Trans.*, 11900 (2013).
[22] A. Núñez-Montenegro, R. Carballo, E.M. Vázquez-López. *Polyhedron*, **27**, 2867 (2008).
[23] R. Carballo, J.S. Casas, E. García-Martínez, G. Pereiras-Gabián, A. Sánchez, J. Sordo, E.M. Vázquez-López, J.C. García-Monteagudo, U. Abram. *J. Organomet. Chem.*, **656**, 1 (2002).
[24] R. Carballo, J.S. Casas, E. García-Martínez, G. Pereiras-Gabián, A. Sánchez, J. Sordo, E.M. Vázquez-López. *Inorg. Chem.*, **42**, 6395 (2003).
[25] A. Núñez-Montenegro, R. Carballo, J.M. Hermida-Ramón, E.M. Vázquez-López. *Polyhedron*, **30**, 2146 (2011).
[26] A. Núñez-Montenegro, R. Carballo, E.M. Vázquez-López. *Polyhedron*, **28**, 3915 (2009).
[27] I. Garcia Santos, U. Abram, R. Alberto, E. Vazquez Lopez, A. Sanchez. *Inorg. Chem.*, **43**, 1834 (2004).
[28] J. Ho, W.Y. Lee, K.J. Tai Koh, P.P. Foo Lee, Y. Yan. *J. Inorg. Biochem.*, **119**, 10 (2013).
[29] L. Otero, G. Aguirre, L. Boiani, A. Denicola, C. Rigol, C. Olea-Azar, J.D. Maya, A. Morello, M. González, D. Gambino, H. Cerecetto. *Eur. J. Med. Chem.*, **41**, 1231 (2006).
[30] S.P. Fricker, R.M. Mosi, B.R. Cameron, I. Baird, Y. Zhu, V. Anastassov, J. Cox, P.S. Doyle, E. Hansell, G. Lau, J. Langille, M. Olsen, L. Qin, R. Skerlj, R.S.Y. Wong, Z. Santucci, J.H. McKerrow. *J. Inorg. Biochem.*, **102**, 1839 (2008).
[31] R. Arancibia, A.H. Klahn, G.E. Buono-Core, E. Gutierrez-Puebla, A. Monge, M.E. Medina, C. Olea-Azar, J.D. Maya, F. Godoy. *J. Organomet. Chem.*, **696**, 3238 (2011).
[32] S.P. Schmidt, W.C. Trogler, F. Basolo. *Inorg. Synth.*, **28**, 160 (1990).
[33] R. Alberto, A. Egli, U. Abram, K. Hegetschweiler, V. Gramlich, A.P. Schubiger. *J. Chem. Soc., Dalton Trans.*, 2815 (1994).
[34] W.J. Geary. *Coord. Chem. Rev.*, **7**, 81 (1971).
[35] (a) A.D. Becke. *Phys. Rev. A*, **38**, 3098 (1988); (b) A.D. Becke. *J. Chem. Phys.*, **98**, 1372 (1993); (c) C. Lee, W. Yang, R.G. Parr. *Phys. Rev. B*, **37**, 785 (1988).
[36] (a) P.J. Hay, W.R. Wadt. *J. Chem. Phys.*, **82**, 270 (1985); (b) P.J. Hay, W.R. Wadt. *J. Chem. Phys.*, **82**, 284 (1985); (c) P.J. Hay, W.R. Wadt. *J. Chem. Phys.*, **82**, 299 (1985).

[37] (a) D. Feller. *J. Comput. Chem.*, **17**, 1571 (1996); (b) K.L. Schuchardt, B.T. Didier, T. Elsethagen, L. Sun, V. Gurumoorthi, J. Chase, J. Li, T.L. Windus. *J. Chem. Inf. Model.*, **47**, 1045 (2007).
[38] (a) J.P. Perdew, K. Burke, M. Ernzerhof. *Phys. Rev. Lett.*, **77**, 3865 (1996); (b) C. Adamo, V. Barone. *J. Chem. Phys.*, **110**, 6158 (1999); (c) A.D. Becke. *J. Chem. Phys.*, **98**, 5648 (1993).
[39] L. Martínez, J.S. Gancheff, F.E. Hahn, R.A. Burrow, R. González, C. Kremer, R. Chiozzone. *Spectrochim. Acta A*, **105**, 439 (2013).
[40] C. Pejo, H. Pardo, A. Mombrú, M.F. Cerdá, J.S. Gancheff, R. Chiozzone, R. González. *Inorg. Chim. Acta*, **376**, 105 (2011).
[41] J.S. Gancheff, P.A. Denis, E.F. Hahn. *J. Mol. Struct. (Theochem)*, **941**, 1 (2010).
[42] J.S. Gancheff, R.Q. Albuquerque, A. Guerrero-Martínez, T. Pape, L. De Cola, F.E. Hahn. *Eur. J. Inorg. Chem.*, **27**, 4043 (2009).
[43] R.E. Easton, D.J. Giesen, A. Welch, C.J. Cramer, D.G. Truhlar. *Theor. Chim. Acta*, **93**, 281 (1996).
[44] (a) M. Dolg, U. Wedig, H. Stoll, H. Preuss. *J. Chem. Phys.*, **86**, 866 (1987); (b) J.M.L. Martin, A. Sundermann. *J. Chem. Phys.*, **114**, 3408 (2001); (c) D. Andrae, U. Häussermann, M. Dolg, H. Stoll, H. Preuss. *Theor. Chim. Acta*, **77**, 123 (1990).
[45] A. Bergner, M. Dolg, W. Kuechle, H. Stoll, M. Preuss. *Mol. Phys.*, **80**, 1431 (1993).
[46] P. Pyykkö. *The Effect of Relativity in Atoms, Molecules and the Solid State*, Plenum, New York (1990).
[47] M.J. Frisch, G.W. Trucks, H.B. Schlegel, G.E. Scuseria, M.A. Robb, J.R. Cheeseman, G. Scalmani, V. Barone, B. Mennucci, G.A. Petersson, H. Nakatsuji, M. Caricato, X. Li, H.P. Hratchian, A.F. Izmaylov, J. Bloino, G. Zheng, J.L. Sonnenberg, M. Hada, M. Ehara, K. Toyota, R. Fukuda, J. Hasegawa, M. Ishida, T. Nakajima, Y. Honda, O. Kitao, H. Nakai, T. Vreven, J.A. Montgomery Jr, J.E. Peralta, F. Ogliaro, M. Bearpark, J.J. Heyd, E. Brothers, K.N. Kudin, V.N. Staroverov, R. Kobayashi, J. Normand, K. Raghavachari, A. Rendell, J.C. Burant, S.S. Iyengar, J. Tomasi, M. Cossi, N. Rega, J.M. Millam, M. Klene, J.E. Knox, J.B. Cross, V. Bakken, C. Adamo, J. Jaramillo, R. Gomperts, R.E. Stratmann, O. Yazyev, A.J. Austin, R. Cammi, C. Pomelli, J.W. Ochterski, R.L. Martin, K. Morokuma, V.G. Zakrzewski, G.A. Voth, P. Salvador, J.J. Dannenberg, S. Dapprich, A.D. Daniels, Ö. Farkas, J.B. Foresman, J.V. Ortiz, J. Cioslowski, D.J. Fox. *GAUSSIAN 09, Rev. A.01*, Gaussian Inc., Wallingford, CT (2009).
[48] C. Hansch, A. Leo. The hydrophobic parameter: measurement and calculation. In *Exploring QSAR. Fundamentals and Applications in Chemistry and Biology*, S.R. Heller (Ed.), pp. 97–124, American Chemical Society, Washington, DC (1995).
[49] H. Cerecetto, R. Di Maio, M. González, M. Risso, P. Saenz, G. Seoane, A. Denicola, G. Peluffo, C. Quijano, C. Olea-Azar. *J. Med. Chem.*, **42**, 1941 (1999).
[50] I. Garcia Santos, U. Abram, R. Alberto, E. Vazquez Lopez, A. Sanchez. *Inorg. Chem.*, **43**, 1834 (2004).
[51] G. Pereiras-Gabián, E.M. Vázquez-López, H. Braband, U. Abram. *Inorg. Chem.*, **44**, 834 (2005).
[52] T. Ghosh, B. Mondal, M. Sutradhar, G. Mukherjee, M.G.B. Drew. *Inorg. Chim. Acta*, **360**, 1753 (2007).
[53] R.W. Balk, D.J. Stufkens, A. Oskam. *J. Chem. Soc., Dalton Trans.*, 1124 (1981).
[54] M.J. Paterson, M.A. Robb, L. Blancafort, A.D. DeBellis. *J. Phys. Chem. A*, **109**, 7527 (2005).
[55] X. Li, D. Zhang, G. Lu, G. Xiao, H. Chi, Y. Dong, Z. Zhang, Z. Hu. *J. Photochem. Photobiol. A: Chem.*, **241**, 1 (2012).
[56] D.R. Gamelin, M.W. George, P. Glyn, F.W. Grevels, F.P.A. Johnson, W. Klotzbucher, S.L. Morrison, G. Russel, K. Schaffner, J.J. Turner. *Inorg. Chem.*, **33**, 3246 (1994).
[57] E.H. Kerns, L. Di. *Drug-like Properties: Concepts, Structure Design and Methods from ADME to Toxicity Optimization*, Academic Press, Amsterdam (2008).